

Theory of Relativistic Electron Beam Bunching by the Wakefield Effects of a Background Plasma

Han S. Uhm

Naval Surface Warfare Center
10901 New Hampshire Ave, White Oak
Silver Spring, Maryland 20903-5000

Abstract

Current profile of a relativistic electron beam is theoretically evaluated in terms of the propagation distance in a chamber containing a diffused plasma, which exerts wakefield effects on the beam. Neglecting the beam erosion and beam loss during the propagation, we find that the beam current profile at a specified propagation distance is expressed only in terms of the time t_0 , at which the beam enters the chamber. Particularly, the current profile has a cusped form at certain time t_0 .

I. INTRODUCTION

When a relativistic electron beam propagates through a preionized plasma channel, channel electrons are expelled by the electrostatic force generated by head of the beam, leaving an ion channel behind. This ion channel partially neutralizes the space charge field of the electron beam, thereby permitting a focused beam. This is beam propagation in the ion-focused-regime (IFR). The beam-ion channel system is often surrounded by a diffuse plasma. When a relativistic electron beam propagates through a IFR channel and a tenuous neutral background plasma, it can expel plasma electrons as well as channel electrons. The plasma electrons move out to the charge neutralization radius a_n where the beam charge is the same as the total enclosed ion charge as shown in Fig. 1. However, in reality, when the plasma electrons are expelled by the beam, they will overshoot the charge neutralization radius and oscillate at a frequency which is usually very close to the electron plasma frequency of the tenuous background plasma. This plasma electron oscillation near the charge neutralization radius produces a wakefield^{1,2} which is electrostatic in nature and has associated electric field components in the radial and axial directions. Particularly, the axial electric field may modulate the beam electron energy along the beam pulse. Implication of the wakefield effects on a long range beam propagation will be studied by this article. We remind the reader that the wakefield effects of a relativistic electron beam propagating through a dense plasma has been extensively studied, in connection with application to the plasma wakefield accelerator³.

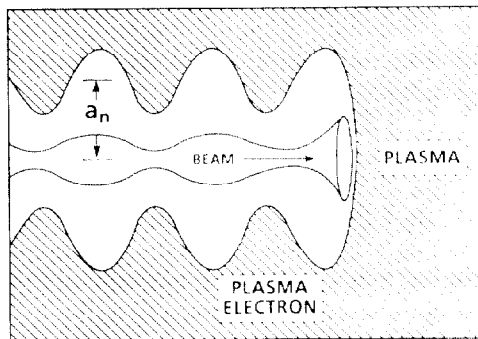


Figure 1. Schematic presentation of the wakefield effects for a relativistic electron beam propagating through a tenuous background plasma. The charge neutralization radius is denoted by a_n .

II. BEAM CURRENT MODULATION

As we have seen in the previous study², the axial electric field of the wakefield is almost a standing wave in the beam frame, thereby modulating the beam electron energy as the beam propagates. In this article, we investigate the energy exchange mechanism between beam segments as the beam propagates, assuming that the axial electric field has a sinusoidal wave form with the axial wavenumber k . Labeling t_0 for the beam segment which exits accelerator at time $t = t_0$, we can express the axial momentum change $\Delta p(z, t_0)$ on this segment as

$$\Delta p(z, t_0) = - \frac{eE_0 z}{\beta_b c} \sin \theta, \quad (1)$$

where $\beta_b c$ is the beam velocity, E_0 is the maximum strength of the wakefield, and $\theta = k\beta_b c t_0$. Equation (1) can also be expressed in terms of the variation of the mass ratio, which is

$$\frac{d\gamma}{dz} = - \frac{eE_0}{mc^2} \sin \theta, \quad (2)$$

where $\theta = \omega t_0$. Here ω is the oscillation frequency of the wakefield waves. Integrating Eq. (2) with respect to z and making use of the initial condition $\gamma = \gamma_b$ at $z = 0$, the mass ratio γ for the beam segment t_0 is given by

This work was supported in part by the Independent Research Fund at the Naval Surface Warfare Center and in part by the Directed Energy Branch in the Strategic Defense Initiative Organization.

$$\gamma = \gamma_b - \frac{eE_0 z}{mc^2} \sin \theta. \quad (3)$$

We also integrate Eq. (2) with respect to t , making use of the initial condition $\gamma = \gamma_b$ at $t = t_0$. The result is

$$\sqrt{\gamma_b^2 - 1} - \sqrt{\gamma^2 - 1} = \frac{eE_0 \sin \theta}{mc\omega} (\phi - \theta), \quad (4)$$

where $\phi = k\beta_b ct = \omega t$. In obtaining Eq. (4), use has been made of $dz/dt = \beta c$ and $\beta = (\gamma^2 - 1)^{1/2}/\gamma$. Differentiating ϕ in Eq. (4) with respect to θ , we find the expression of $d\phi/d\theta$

$$\left(\frac{d\phi}{d\theta} - 1\right) \tan \theta = \theta - \phi + \frac{\omega}{\beta c} z. \quad (5)$$

Defining

$$\xi(\theta) = \frac{eE_0 \omega z^2}{2\gamma^2(\theta) \gamma_b mc^3}, \quad (6)$$

we can show that Eq. (5) is simplified to

$$\frac{d\phi}{d\theta} = 1 + \xi \cos \theta, \quad (7)$$

in the limit of a relativistic electron beam characterized by $\gamma \gg 1$. In Eq. (7) the relativistic mass ratio $\gamma(\theta)$ has been obtained in Eq. (3). Note that the beam current $I_b(t_0)$ enters continuously through the chamber entrance located at $z = 0$ and time $t = t_0$. When this beam segment arrives at $z = z$ in time t , this beam segment is stretched by a factor of dt/dt_0 . Therefore, the beam current of the segment t_0 at z is proportional to the factor of $d\theta/d\phi$. The ratio of the input to output current is expressed as

$$\frac{I(\theta)}{I_b(\theta)} = \alpha \frac{N(z)}{|d\theta/d\phi|}, \quad (8)$$

where the normalization factor N is defined by

$$\frac{2\pi}{N(z)} = \int_0^{2\pi} |d\theta/d\phi| d\theta, \quad (9)$$

and $d\phi/d\theta$ is obtained from Eq. (5), together with Eqs. (3) and (4), for a specified value of θ . In Eq. (8), the parameter α represents the loss factor of the beam during the propagation, which is in the range of $0 < \alpha < 1$. In obtaining Eq. (8), we have assumed following: First, beam-head erosion is negligibly small. In many present experiments, the beam-head erosion is not necessarily small. Second, although beam segments can be stacking up to each other, the beam segments do not cross each other. In real

situation, they do cross each other. For example, later segment can bypass previous one. Third, the beam segment gains or loses energy according to a predetermined sinusoidal wave. In a real case, the energy-gain mechanism of a beam segment may be much more complicated than a simple sinusoidal wave pattern. For example, for a long risetime beam, the first peak of the electric field occurs at a considerably later segment of the beam and this peak value is unusually larger than the following peak values². Of course, these detail properties can be also incorporated into the theory if needed. However, the simple theoretical description in this article provides a basic understanding of the beam current profile at the propagation distance z .

Substituting Eq. (6) into Eq.(7) and carrying out a straightforward calculation, we obtain

$$\frac{d\phi}{d\theta} = 1 + \frac{eE_0 \omega z^2}{2\gamma_b mc^3} f(\theta), \quad (10)$$

where the function $f(\theta)$ is defined by

$$f(\theta) = \frac{\cos \theta}{\gamma^2}, \quad (11)$$

and the relativistic mass ratio γ is expressed as Eq. (3). We find from Eq. (11) that the minimum value f_{\min} of the function $f(\theta)$ occurs at the parameter $\theta = \theta_0$ satisfying

$$\sin \theta_0 = \sqrt{\left(\frac{\gamma_b mc^2}{2eE_0 z}\right)^2 + 2} - \frac{\gamma_b mc^2}{2eE_0 z}, \quad (12)$$

which is a function of the propagation distance z .

One of the solutions to Eq. (12), which is in the range $\pi/2 < \theta_0 < \pi$ ensures the minimum value f_{\min} with the negative sign. We therefore note from Eqs. (8) and (11) that the maximum output current occurs at $\theta = \theta_0$, which is less than π and larger than $\pi/2$. We also note that if the value of $eE_0 \omega z^2 f_{\min} / 2\gamma_b mc^2$ is less than -1, the output current has two peaks in the range of θ satisfying $\pi/2 < \theta < 3\pi/2$. It is also noted from Eq. (12) that the parameter θ_0 decreases from $\theta_0 = \pi$ to $\theta_0 = \pi/2$ as the value of the parameter $eE_0 z / \gamma_b mc^2$ increases from zero to unity. However, the value of the parameter $eE_0 z / \gamma_b mc^2$ is not allowed to be more than unity because of violation of the beam equilibrium condition.

As an example of comparison between the theoretical model discussed in this article and a particle simulation study, we consider the case of the plasma density $n_p = 4 \times 10^9$ electrons cm^{-3} , which ensures the wakefield frequency $\omega = 2.86 \times 10^9$ rad/sec. The beam energy is 4.5 MeV corresponding to $\gamma_b = 10$. The beam current and risetime are 2 kA and 1 ns, respectively. The fractional charge

neutralization of the ion channel is $f_c = 0.5$. Making use of these information, we find the maximum axial electric field $E_0 = 10$ kV/cm from theoretical calculation^{1,2}. The chamber length is 4 m. These system parameters are identical to the simulation study presented in Fig. 15 in the reference 2. Substituting necessary information into Eq. (12), we find that the maximum output current occurs at $\theta_0 = 2n\pi + 1.973$, where $n = 0, 1, 2, \dots$, and that the corresponding value of the parameter $eE_0\omega z^2 f_{\min}^2 / 2\gamma_b mc^2$ is -0.84, which is still larger than -1, ensuring a single peak of the output current per each oscillation period.

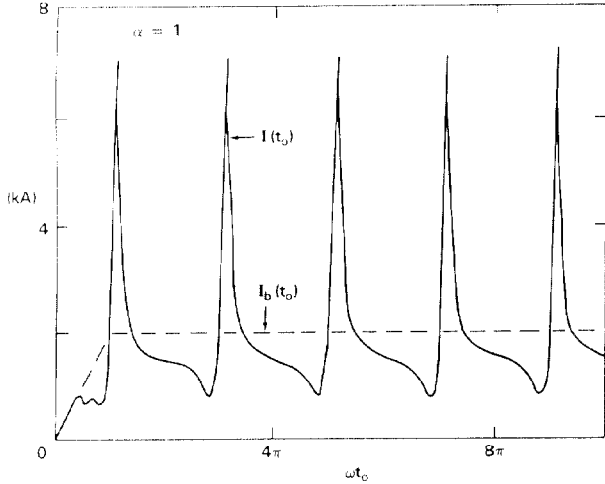


Figure 2. Plots of the input (dashed line) and output (solid line) current profiles versus ωt_0 from Eqs. (3), (8), (10), and (11) for $\alpha = 1$, $n_p = 4 \times 10^9 \text{ cm}^{-3}$, $\gamma_b = 10$, $I_b = 2 \text{ kA}$, $f_c = 0.5$ and the input risetime $t_r = 1 \text{ ns}$.

Assuming that the input beam has a linear risetime t_r , when the beam current rises linearly in time and then remain constant at the plateau value, we remind the reader that the beam and ion channel system exhibits a net negative charge after the time $f_c t_r$, where f_c is the charge neutralization factor of the ion channel. Therefore, there is a delay from the beam front, in setting up the wakefield waves on the beam. In this context, the parameter θ must be redefined by $\theta = \omega(t_0 - f_c t_r)$. Shown in Fig. 2 are plots of the input (dashed lines) and output (solid curve) currents versus ωt_0 . The output current profile is obtained from Eqs. (3), (8), (10) and (11) for $\alpha = 1$ corresponding to the case of no beam electron loss. The normalization factor N is calculated to be $N = 0.756$. Comparing the output current profile in Fig. 2 with Fig. 15b in the reference 2, we note that results of the theoretical model agree remarkably well with the simulation data. For a long propagation distance (i.e., $z = 8 \text{ m}$ in Fig. 15c in reference 2), we can numerically obtain the output current profile from Eq. (8), together with Eqs. (3), (4) and (5), which may exhibits two peaks in each oscillation period.

In the limit when the relativistic mass ratio γ in Eq. (11) is so large that it is approximated by $\gamma = \gamma_b$, the ratio of the input to output current is simplified to

$$\frac{I(t_0)}{I_b(t_0)} = \frac{\alpha \sqrt{|1 - \xi^2|}}{|1 + \xi \cos \theta|}, \quad (13)$$

where the parameter ξ defined in Eq. (6) is approximated by

$$\xi = \frac{\omega z e E_0 z}{2\gamma_b^3 mc^3}. \quad (14)$$

The output beam current $I(t_0)$ has sharp peaks at $\theta = (2n + 1)\pi$, where $\cos\theta$ is the negative unity. Because of the functional form of $1 + \xi \cos\theta$, the output beam current at z has a cusped form near the parameter $\theta = (2n + 1)\pi$, which is distinctively different from a sinusoidal wave form.

We define the critical propagation distance z_c

$$z_c = \sqrt{\frac{2\gamma_b^3 mc^3}{eE_0\omega}}, \quad (15)$$

by making use of Eq. (14). From the discussion in the previous paragraph and Eq. (13), it is obvious that the bunching mechanism of the electron beam makes one peak per each period until the beam segment t_0 reaches $z = z_c$. If the beam propagates further distance than z_c , it starts to bunch two peaks per each period, thereby breaking further the beam into small beamlets. Symptoms of this behavior have been observed in a particle simulation study² of a long range beam propagation.

III. CONCLUSIONS

Current profile of a relativistic electron beam has been theoretically investigated in terms of the propagation distance in a chamber containing a diffused plasma, which exerts wakefield effects on the beam electrons. For a highly relativistic beam, we found that the beam current profile at the propagation distance z is inversely proportional to the factor of $1 + \xi \cos \theta$, where $\theta = \omega t_0$, and where the parameter ξ is proportional to the strength of the wakefield waves and proportional to the square of the propagation distance. Therefore, the current profile has a cusped form at the parameter $\theta = \pi$.

IV. REFERENCES

- [1] H. S. Uhm, "Wakefield Theory of a Relativistic Electron Beam", *Phys. Lett. A*, **149**, 469 (1990).
- [2] H. S. Uhm and G. Joyce, "Theory of Wakefield Effects of a Relativistic Electron Beam Propagating in a Plasma", *Phys. Fluids*, in press (1991).
- [3] P. Chen, J. M. Dawson, R. W. Huff and T. Katsouleas, *Phys. Rev. Lett.* **54**, 693 (1985).